# TURBULENT FLOW IN A SPRAY DRYING CHAMBER

HIROMOTO USUI, YUJI SANO, YOSHIHIRO YANAGIMOTO
AND YOSHITO YAMASAKI
*Department of Chemical Engineering, Yamaguchi University, Ube 755*

*Key Words*: Drying, Spray Dryer, Turbulent Flow, Recirculating Flow

**Turbulent flow in a spray drying chamber was analysed experimentally. Instantaneous fluctuating velocity was measured by a hot-wire anemometer with a split-film probe. This measurement enabled us to obtain the correct velocity field in the chamber without atomization. The turbulent fluctuation in the spray drying chamber was extremely larger than the usual turbulent level of free jet or tube flow. It is suggested that the large fluctuation can be attributed to the unsteady nature of the downward jet, caused by the interaction between the shape of the chamber and the downward jet.**

## Introduction

Spray drying is a chemical engineering operation of growing importance. Many types of spray dryers are available, and each seems to satisfy its first object, i.e. to produce dried materials successfully. However, spray dryer design and operation is not well understood. Very complicated droplet trajectories and their interaction with the air flow prevent us from making a simple design scheme for various types of spray dryer. Many studies have been devoted to solving this quite complicated problem. Among others, Gauvin *et al.*[1,5,7,10] developed a design scheme which was essentially based on the trajectory of a particle flying within an experimentally known flow field in a spray drying chamber. Crowe[3] recently reviewed the modeling of spray-air contact in spray drying systems. Crowe *et al.*[4] proposed a PSI-Cell model in which the interactions between droplets and air for momentum, heat and mass transfer were included. However, the practical application of the model is limited to a simple tube-type dryer. Pham and Keey[12] analyzed the drying behaviour of particles in the jet zone of a spray dryer. They used a modified velocity profile based on the single-phase submerged jet. A similar treatment was made by Miura and Ohtani.[11] Goffred and Crosby[6] have recently developed the limiting analytical relationships for prediction of spray dryer performance. Two limiting conditions, i.e. completely mixed flow and plug flow, were considered to give an estimation of drying performance.

The characteristics of atomizers are, of course, important, and many previous investigations (e.g. Kim and Marshall[8] and Crosby[2]) are available. It is evident that there exist droplet-gas interactions. Thus the most sophisticated design scheme will be obtained by using an elaborated model like the PSI-Cell model[4] for various dryer configurations. But this is difficult except for a simple form of dryer such as a tube-type dryer. Otherwise, the simplest model of Goffred and Crosby[6] would be most adequate for the practical problem of spray dryer performance. Although the recent development of turbulence modeling is remarkable, the accuracy of predicted results in a complex flow system like the spray dryer used in this study is still open to question. Thus it may be important and most helpful for practical spray dryer design to obtain precise measurements of flow characteristics in the spray drying chamber. In this report, as the first step in flow measurement, a spray dryer without an atomizer was constructed, and a hot-wire anemometer with a split-film probe was used to detect the air velocity.

The spray dryer of this study is a prototype model of a commercial dryer. The purposes of the study are two. The first is to develop time-smoothed velocity profiles in the spray drying chamber. This result will enable us to carry out the calculation of heat and mass transfer between droplets and air flow. The second purpose is to obtain the turbulent flow characteristics in the spray drying chamber. The results will be used to check the effectiveness of turbulence models such as the $k-\varepsilon$ model in future studies.

## 1. Experimental

The chamber used in this work (**Fig. 1**) consists of a cylindrical section, 942 mm in diameter by 2150 mm long, with a conical bottom 650 mm long. The air is supplied through a horizontal tube, a 90-degree elbow and a vertical tube, 400 mm in diameter and 800 mm long. A section converging from 400 mm to 250 mm in diameter follows. After the flow is converged, the inlet tube, 250 mm in diameter and 500 mm long, conducts the flow into the chamber. The upper half of the inlet

Received September 10, 1984. Correspondence concerning this article should be addressed to H. Usui. Y. Yanagimoto is now with Sanyo Kasei Co., Ltd.

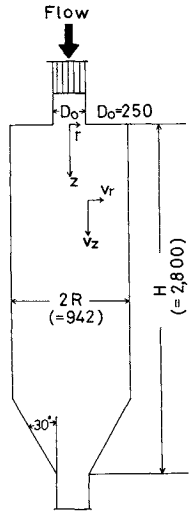


**Fig. 1.** Spray chamber.

tube contains a honeycomb as a flow straightener. The inlet air flow has no swirling velocity component. Although it is possible to install a spray nozzle on this experimental apparatus, it is very difficult to measure the velocity in the droplet-air two-phase flow. Thus, in this study, no spray nozzle was installed. The average velocity of inlet jet, $U_o$, was a fixed value of 7.55 m/s, and the Reynolds number based on the inlet condition was $1.26\times10^5$. A constant-temperature hot-wire anemometer was used to measure the local velocity in the chamber. Since, in preliminary experiments with the flow visualization technique, a strong recirculating flow near the wall was observed, a split-film probe (Kanomax, model 128810) was used to detect the instantaneous velocity component and its direction in the recirculating zone. The output of the hot-wire anemometer was A–D converted by TEAC, DR-2000, and statistical turbulence analysis was performed by means of an ACOS-800 computer system. The sampling frequency and the data size were 200 Hz and $10^4$ respectively.

## 2. Results and Discussion

The inlet flow conditions (mean velocity profile and turbulent intensity distributions) are shown in **Figs. 2** and **3**. The time-smoothed velocity profile at the inlet section is in good agreement with the well-known velocity profile in fully developed turbulent tube flow. The turbulent intensity data are compared with the experimental results by Lawn[9] in Fig. 3. The turbulent intensity in this work is a little lower than the well-accepted data for turbulent tube flow, except in the center portion of the inlet tube. This may be caused by the converging section and the honeycomb which were located upstream of the inlet section.

The output signals of the split-film probe were analyzed to give the instantaneous axial velocity component and its flow direction. The time-smoothed

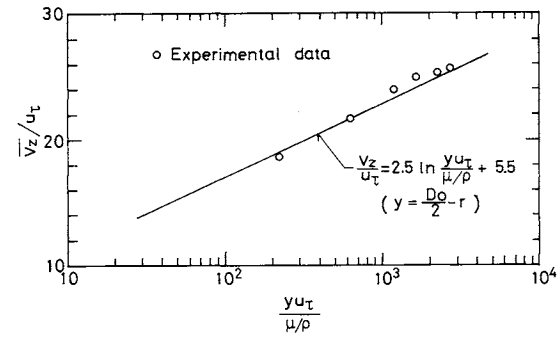


**Fig. 2.** Distribution of axial time-smoothed velocity at inlet section ($z/H=-0.01$).

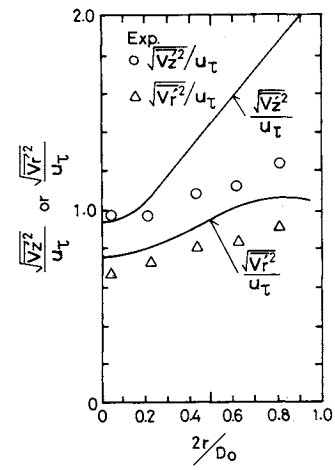


**Fig. 3.** Distribution of turbulent intensity at inlet section ($z/H=-0.01$).

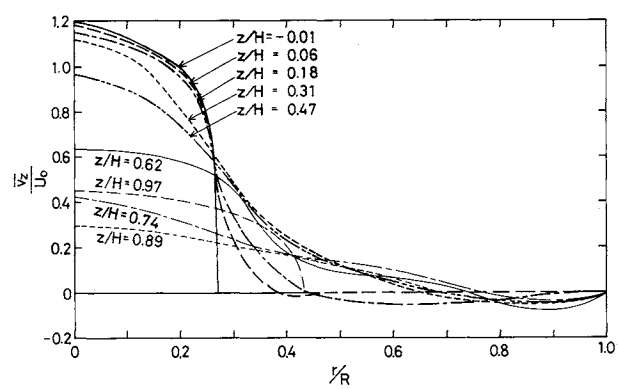


**Fig. 4.** Distributions of axial time-smoothed velocity.

velocity distribution in the axial direction is shown in **Fig. 4**. From the equation of continuity, the radial velocity was calculated by

$$\overline{v_r}=-\frac{1}{r}\int_0^r r\left(\frac{\partial\overline{v_z}}{\partial z}\right)dr \qquad (1)$$

The results are shown in **Fig. 5**. These results can be used for the further analysis of droplet trajectory and heat and mass transfer between droplets and air flow. To illustrate the flow pattern in the spray dryer, the time-smoothed velocities at several cross sections are shown vectorially in **Fig. 6**-a. The inlet jet consists of a

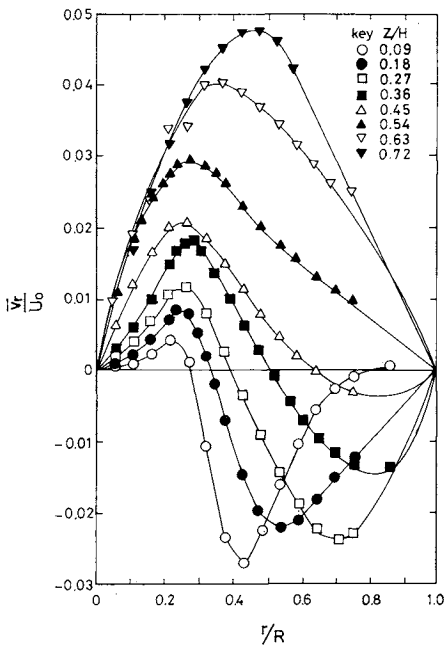


Fig. 5. Distributions of radial time-smoothed velocity.

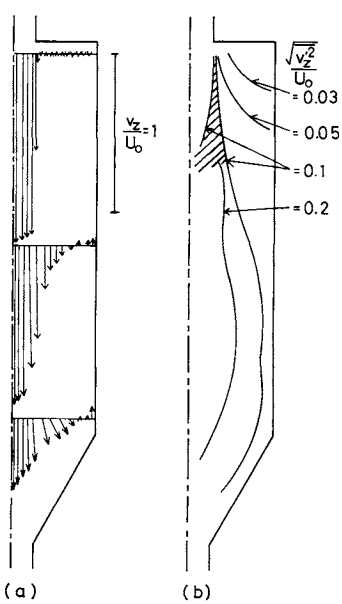


Fig. 6. Distributions of time-smoothed velocity and turbulent intensity.

typical jet zone around the centerline of the chamber. The flow in the chamber seems to be subdivided into two zones, i.e. the inner jet zone around the centerline and the outer calm zone where the time-smoothed velocity is very small. There exists a wide zone near the side wall where the average axial velocity is weakly negative. This means that a recirculating flow exists in this zone, in which the fluctuating velocity is predominant. The boundary between the jet zone and the recirculating zone is easily determined by the flow-visualizing technique. The tuft method was used in this study. The solid symbol, ●, in **Fig. 7** shows the position where the tuft begins to fluctuate upward.

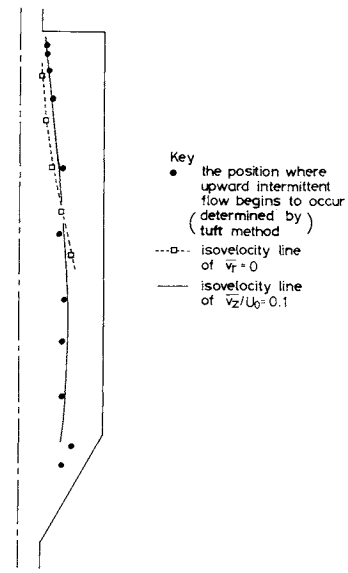


Fig. 7. Boundary of recirculation zone determined by tuft method and its comparison with results of velocity measurements.

The open square shows the position where the radial velocity component becomes zero as shown in Fig. 5. The zone just outside of this key is interpreted as a zone where the entrainment flow is remarkable. These two experimentally determined boundaries correspond well to the isovelocity line of $v_z/U_o=0.1$.

The radial velocity distributions shown in Fig. 5 indicate that there exists a negative radial velocity in the recirculating zone of the upper side if $z/H<0.4$. This means that the entrainment by the inlet jet causes a centerward air flow in the recirculating zone of this portion. In the lower side of the recirculating zone ($z/H>0.4$), the downward jet spreads out and the radial velocity has a positive value almost throughout the cross section.

Figure 6-b shows the turbulent intensity profile normalized by the inlet velocity. As shown in Fig. 3, the turbulent intensity in the inlet jet is rather small, and its value is several percent of $U_o$. Turbulence is generated in the hatched portion of this diagram surrounded by the two isointensity lines of $\sqrt{v_z'^2}/U_0=0.1$. Turbulence is amplified downstream. Maximum turbulence intensity, 20% of $U_o$, was observed on the centerline at $z/H=0.6$. Usually, such a large turbulent intensity cannot be measured correctly because of the nonlinearity of the hot-wire anemometer. No correction of the output data of the hot-wire anemometer was made in this study. However, as pointed out a little later, the extremely large value of turbulent intensity is caused by the intermittent flow characteristics with lower frequency. Thus the present results of turbulent intensity measurements are judged to be correct enough to figure out the flow characteristics in a spray drying chamber. The region near the upper

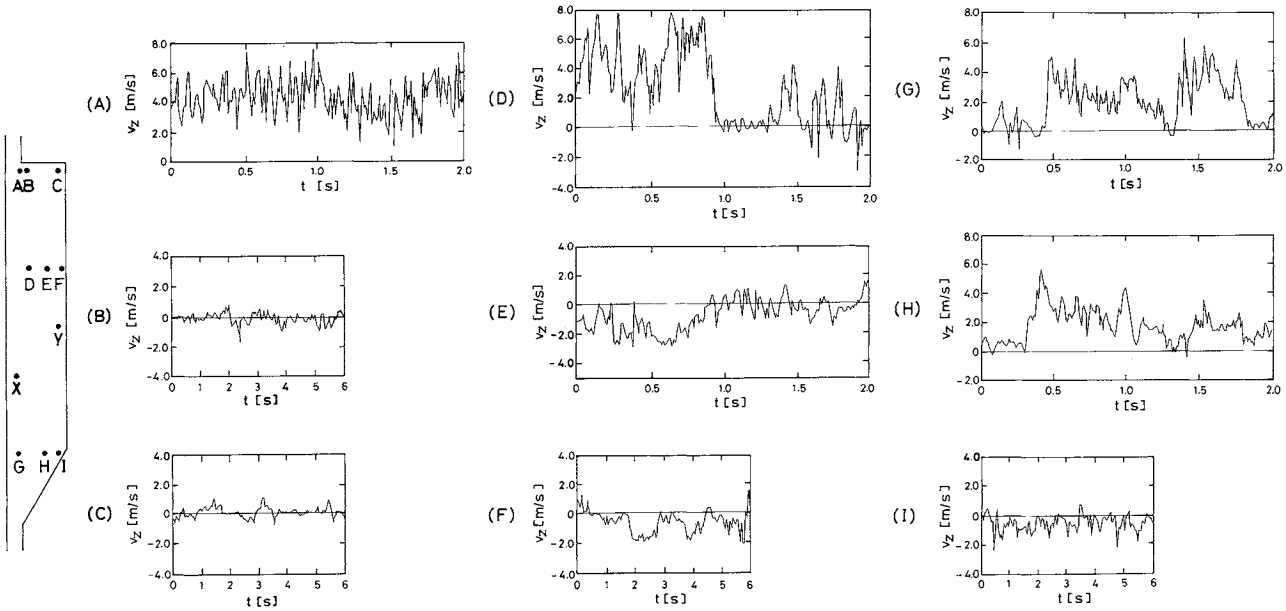


**Fig. 8.** Velocity fluctuations at various positions in spray chamber.

plate, i.e. that surrounded by the region near the upper plate, i.e. that surrounded by the line of $\sqrt{v_z'^2}/U_o = 0.03$ and the solid walls in Fig. 6-b, shows a very calm zone. In this region, the time-smoothed velocity is almost zero, and the turbulent intensity is less than 3% of $U_o$. This region seems to be preferable to avoid the adhesion of undried particles to the wall in the recirculating zone.

In the region near the side wall, except the near upper plate region mentioned above, the turbulent intensity is relatively high, while the time-smoothed velocity is a very small negative value from Figs. 4 and 6-b.

To obtain more detailed information of flow characteristics, the fluctuating velocity data are shown in **Fig. 8** against real time. The symbols (A)–(I) correspond to the measuring positions indicated in Fig. 8. Point (A) is located just inside the inlet jet boundary, and the results shown in Fig. 8-A indicate that the air flows downward all the time. Point (B) is located just outside the inlet jet, and point (C) is located at the calmest region near the corner. As shown in Figs. 8-B and 8-C, flow is almost stagnant near the upper plate.

Position (D) is thought to be included in the downward jet. However, Fig. 8-D clearly shows intermittent flow behaviour. Intermittent upward flow is clearly observed in the recirculating zone (see Figs. 8-E and 8-F). The autocorrelation curve of the fluctuating velocity at position (F) is shown in **Fig. 9**. This diagram shows a remarkable peak at delay time $\tau =$ 1.05 s. Thus the upward recirculating flow along the side wall is observed at one-second intervals at a fixed point, and its velocity is typically observed as around

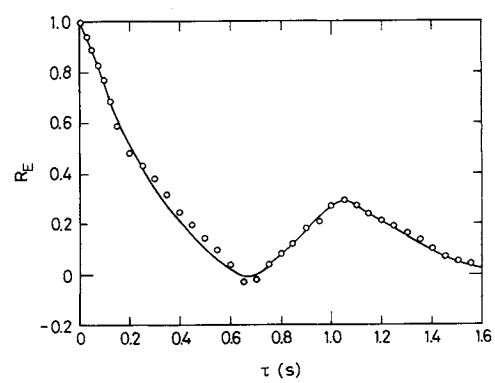


**Fig. 9.** Eulerian autocorrelation coefficient at position (F).

2 m/s from Fig. 8-F. In Figs. 8-G and 8-F, an almost stagnant period, i.e. an almost zero-velocity period, is sometimes observed in this diagram. The same intermittency is also observed in Fig. 8-D. The stagnant periods continue around 0.3–0.5 s. This rather long period prevents us from regarding this intermittency as caused by the entrainment flow induced by the ring vortex of the inlet jet. Also, it was confirmed by measuring the inlet velocity at the entrance section that the inlet jet was steady. Thus the reason for this remarkable intermittency is supposed to be the radial fluctuation of the center position of the downward jet. The downward jet is supposed to have an essentially unsteady nature, and it hits the side wall at the conical bottom of the chamber. Thus, the locally induced upward flow penetrates into the recirculating zone strongly along the side wall. This flow behaviour is indirectly supported by the result of space-time correlation measurement. The space-time correlation coefficient, $R_{XY}$, is defined by

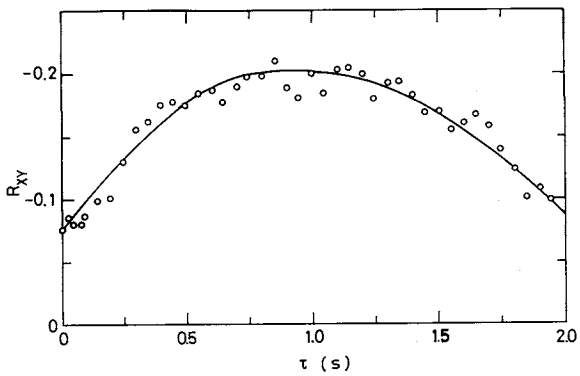


**Fig. 10.** Space-time correlation coefficient measured at positions (X) and (Y) shown in Fig. 5.

$$R_{XY}=\frac{\overline{v'_z(t)_{\text{at }X}\, v'_z(t+\tau)_{\text{at }Y}}}{\sqrt{\overline{v'^2_{z\ \text{at }X}}}\sqrt{\overline{v'^2_{z\ \text{at }Y}}}} \tag{2}$$

and positions (X) and (Y) are indicated in Fig. 8. In this case, two I-probes were used in hot-wire anemometry. The result of space-time correlation is shown in **Fig. 10**. This diagram indicates that $R_{XY}$ has the maximum value at $\tau=1$ s. This means that the fluid element observed as the downward high-velocity element at position (X) is observed 1 s later at position (Y) as the upward recirculating flow after it hits the side wall at the conical bottom of the chamber. The fluid pass is supposed to be (X)→(H)→(Y), typically. This distance is approximately 2 m. On the other hand, the velocity of the upward recirculating flow is observed as 2 m/s from Fig. 8-F. Also, the velocity of the downward jet at (X) is about 2–4 m/s. The above-mentioned conditions mean that the fluid element at (X) is supposed most probably to pass position (Y) around 0.5–1.0 s later, corresponding well to the observation in Fig. 10. According to the discussion given above, it may be concluded that there exists intermittently a strong upward recirculating flow along the side wall of the spray drying chamber.

## 3. Conclusion

Turbulent flow and mixing in a spray drying chamber was analyzed experimentally. The complex flow configuration in a spray chamber without atomizer has been considerably clarified. In particular, a set of quantitative data of both axial and radial velocity distribution was obtained. These experimental results will be useful for future of spray dryer modeling. The turbulent fluctuation in the spray chamber was extremely larger than the usual turbulence level of free jet or tube flow. It is suggested that the large fluctuation was caused by the unsteady, or intermittent, nature of the downward jet.


### Acknowledgment

This work was partially supported by a Grant-in-Aid (No. 56550676) from the Ministry of Education, Science and Culture of Japan, for which the authors express their thanks. They also express their appreciation to Dr. H. Hayashi, Snow Brand Milk Products Co., Ltd., for his valuable suggestion and discussion about the configuration of the spray drying chamber. The authors also appreciate the experimental cooperation of I. Mihata and K. Katoh.


### Nomenclature

| | | | |
|---|---|---|---|
| $D_o$ | = | inlet diameter of spray chamber | [m] |
| $H$ | = | height of spray chamber | [m] |
| $R$ | = | inner diameter of spray chamber | [m] |
| $Re$ | = | Reynolds number at inlet section | [—] |
| $R_{XY}$ | = | space-time correlation coefficient | [—] |
| $r$ | = | radial coordinate defined in Fig. 1 | [m] |
| $t$ | = | time | [s] |
| $U_o$ | = | space-averaged velocity at inlet section | [m/s] |
| $u_\tau$ | = | wall shear velocity | [m/s] |
| $\overline{v_r}$ | = | radial component of time-smoothed velocity | [m/s] |
| $v_z$ | = | instantaneous velocity in axial direction | [m/s] |
| $\overline{v_z}$ | = | axial component of time-smoothed velocity | [m/s] |
| $v'_z$ | = | fluctuating velocity in axial direction | [m/s] |
| $z$ | = | axial coordinate defined in Fig. 1 | [m] |
| $\mu$ | = | viscosity | [Pa·s] |
| $\rho$ | = | density | [kg/m$^3$] |
| $\tau$ | = | delay time | [s] |

### Literature Cited


1) Baltas, L. and W. H. Gauvin: *AIChE J.*, **15**, 764 (1969).
2) Crosby, E. J.: Proc. 1st Int. Conf. on Liquid Atomization and Spray Systems, Tokyo (1978).
3) Crowe, C. T.: "Advances in Drying," A. S. Mujumdar, ed., Vol. 1, p. 63, Hemisphere Pub., New York (1980).
4) Crowe, C. T., M. P. Shama and D. E. Stock: *J. Fluid Eng.*, **99**, 326 (1977).
5) Gauvin, W. H. and S. Katta: *AIChE J.*, **22**, 713 (1976).
6) Goffredi, R. A. and E. J. Crosby: *I&EC Process Des. Dev.*, **22**, 665 (1983).
7) Katta, S. and W. H. Gauvin: *AIChE J.*, **21**, 143 (1975).
8) Kim, K. Y. and W. R. Marshall, Jr.: *AIChE J.*, **17**, 575 (1971).
9) Lawn, C. J.: *J. Fluid Mech.*, **48**, 477 (1971).
10) Manning, W. P. and W. H. Gauvin: *AIChE J.*, **6**, 184 (1960).
11) Miura, T. and S. Ohtani: *Kagaku Kogaku Ronbunshu*, **5**, 130 (1979).
12) Pham, Q. T. and R. B. Keey: *Trans. Instr. Chem. Engrs.*, **55**, 114 (1977).